Dynamic Reconfiguration of Distribution Network Systems: A Key Flexibility Option for RES Integration

F.V. Dantas[1], D.Z. Fitiwi[2], S. F. Santos[2], J.P.S. Catalão[1,2,3]
INESC TEC and FEUP[1], Porto, C-MAST/UBI[2], Covilhã, INESC-ID/IST-UL Lisbon[3], Portugal
flaviovd94@gmail.com; dzf@ubi.pt; sdfsantos@gmail.com; catalao@fe.up.pt

***Abstract*—The growing trend of variable energy source integration in power systems (especially at a distribution level) is leading to an increased need for flexibility in all levels of the energy flows in such systems: the supply, the network and the demand sides. This paper focuses on a viable flexibility option that can be provided by means of a dynamic network reconfiguration (DNR), an automatic changing of line statuses in response to operational conditions in the system. The ultimate aim is to assess the impacts of such flexibility on the utilization levels of variable power sources (mainly, solar and wind) integrated at a distribution level. To perform this analysis, a stochastic mixed integer linear programming (S-MILP) operational model is developed in this work. The objective of the optimization problem is to minimize the sum of the most relevant cost terms while meeting a number of model constraints. The proposed model dynamically finds an optimal configuration of an existing network system in accordance with the system's operational conditions. The operation scale in the current work is one day, but with the possibility of an hourly reconfiguration. The standard IEEE 41-bus system is employed to test the proposed model and perform the analysis. Numerical results generally show that DNR leads to a more efficient utilization of renewable type DGs integrated in the system, reduced costs and losses, and a substantially improved system performance especially the voltage profile in the system.**

Keywords—Distributed generation; network reconfiguration; renewable energy sources; stochastic mixed integer linear programming;

I. NOMENCLATURE

A. Sets/Indices

c/Ω^c	Index/set of capacitor banks
es/Ω^{es}	Index/set of energy storage
g/Ω^g	Index/set of generators
h/Ω^h	Index/set of hours
l/Ω^l	Index/set of lines
$n,m/\Omega^n$	Index/set of buses
s/Ω^s	Index/set of scenarios
$\varsigma/\Omega^\varsigma$	Index/set of substations
Ω^1/Ω^0	Set of normally closed/opened lines

B. Parameters

$E_{es,n,s,h}^{min}, E_{es,n,s,h}^{max}$	Energy storage limits (MWh)
$ER_g^{DG}, ER_\varsigma^{SS}$	Emission rates of DGs and energy purchased, respectively (tCO_2e/MWh)
g_l, b_l, S_l^{max}	Conductance, susceptance and flow limit of line l, respectively (Ω^{-1}, Ω^{-1}, MVA)
OC_g	Cost of unit energy production ($€/MWh$)
pf_g, pf_{ss}	Power factor of DGs and substation
$P_{g,n}^{DG,min}, P_{g,n}^{DG,max}$	Power generation limits (MW)
$P_{es,n}^{ch,max}, P_{es,n}^{dch,max}$	Charging/discharging upper limit (MW)
$PD_{s,h}^n, QD_{s,h}^n$	Demand at node n (MW, MVAr)
$Q_{c,n,s,h}^{c,0}$	Block of capacitor bank (MVAr)
R_l, X_l	Resistance, and reactance of line l (Ω, Ω)
SW_l	Cost of line switching €/switch
V_{nom}	Nominal voltage (kV)
$\eta_{es}^{ch}, \eta_{es}^{dch}$	Charging/discharging efficiency
λ^{CO_2}	Cost of emissions ($€/tCO_2e$)
λ^{es}	Variable cost of storage system ($€/MWh$)
λ_h^ς	Price of electricity purchased
μ_{es}	Scaling factor (%)
$\upsilon_{s,h}^P, \upsilon_{s,h}^Q$	Unserved power penalty ($€/MW, €/MVAr$)
ρ_s	Probability of scenario s

C. Variables

$E_{es,n,s,h}$	Reservoir level of ESS (MWh)
$I_{es,n,s,h}^{ch}, I_{es,n,s,h}^{dh}$	Charging/discharging binary variables
$P_{g,n,s,h}^{DG}, Q_{g,n,s,h}^{DG}$	DG power (MW, MVAr)
$P_{es,n,s,h}^{ch}, P_{es,n,s,h}^{dch}$	Charged/discharged power (MW)
$P_{\varsigma,s,h}^{SS}, Q_{\varsigma,s,h}^{SS}$	Imported power from grid (MW, MVAr)
$P_{n,s,h}^{NS}, Q_{n,s,h}^{NS}$	Unserved power (MW, MVAr)
$P_{l,s,h}, Q_{l,s,h}$	Power flow through a line l (MW, MVAr)
$PL_{l,s,h}, QL_{l,s,h}$	Power losses in each feeder (MW, MVAr)
$Q_{c,n,s,h}^c$	Reactive power injected by SCBs (MVAr)
$x_{c,n,h}$	Integer variable of capacitor banks
$x_{l,h}$	Binary switching variable of line l
$\Delta V_{n,s,h}, \Delta V_{n,s,h}$	Voltage deviation magnitude (kV)
$\theta_{l,s,h}$	Voltage angles between two nodes line l

D. Functions

$EC^{DG}, EC^{ES}, EC^{SS}$	Expected cost of energy produced by DGs, supplied by ESSs and imported (€)

This work was supported by FEDER funds through COMPETE 2020 and by Portuguese funds through FCT, under Projects SAICT-PAC/0004/2015 - POCI-01-0145-FEDER-016434, POCI-01-0145-FEDER-006961, UID/EEA/50014/2013, UID/CEC/50021/2013, and UID/EMS/00151/2013. Also, the research leading to these results has received funding from the EU Seventh Framework Programme FP7/2007-2013 under grant agreement no. 309048.

978-1-5386-3917-7/17/$31.00 ©2017 IEEE

$EmiC^{DG}, EmiC^{SS}$	Expected emission costs of power produced by DGs and imported from the grid (€)
$ENSC$	Expected cost for unserved energy (€)
SWC	Cost of line switching (€)

II. Introduction

Electrical distribution systems need to cope up with challenges induced by the increasing global concerns on environmental change and energy security among others. All this is driving the evolution of existing distribution network systems into smarter ones. Smart network systems are expected to be equipped with advanced technologies such as emerging flexibility options that can support the integration and effective utilization of non-conventional energy sources such as wind and solar. Such energy resources are particularly gaining interest globally, and their share in the final energy delivery is growing dramatically [1], [2]. This development will be further accelerated following the favorable agreement of states to curb global warming and mitigate climate change. Many policy makers across the globe are now embarking on ambitious sustainable energy production targets [3], [4].

However, increased level of variable renewable energy sources (vRESs) such as wind and solar comes with certain challenges [5] mainly due to their intermittent nature. This increases uncertainty and variability in the system, leading to technical problems and enormous difficulty in the critically important minute-by-minute balancing requirement of supply and demand. Particularly, at distribution levels, there is little room for any compromise on the stability and integrity of the system as well as the reliability and quality of power delivered to the end-users. Generally, the intermittent nature of such resources (vRESs) substantially increases the flexibility needs in the system. Flexibility in this paper should be understood as the capability of the system to balance variations in the demand and supply sides. Traditionally, this has been mostly handled by the supply side i.e. any variation in demand has been instantly balanced by generators designed for this purpose. However, this norm is nowadays changing, where flexibility options that can be provided by the supply, demand, network and/or other means are largely sought.

This paper focuses on a viable flexibility option that can be provided by means of a dynamic network reconfiguration (DNR). DNR deals with a continuous and automated change of line statuses depending on the operational conditions in the distribution system. This should generally lead to a more efficient operation of the system by maximizing the utilization level of variable energy resources (mainly, wind and solar), and minimizing their side effects such as voltage rise issues.

References [6], [7] present a detailed review of the most relevant works in the subject area of distribution network reconfiguration by mainly focusing on the methods employed to handle the resulting optimization problem, and the main objectives of carrying out such an optimization. Generally, the purpose of reconfiguration in existing studies has been mainly to minimize network losses [8], [9], [10], [11]. However, a properly (optimally) executed network reconfiguration can simultaneously meet a number of additional objectives such as improving the voltage profile and reliability in the system [12], [13], [14], [15]. In addition, a more frequent reconfiguration (which is alternatively called an intelligent reconfiguration) can substantially enhance the flexibility of existing systems, paving the way to an increased penetration and use levels of vRESs. Authors in [16] propose a joint optimization model for simultaneously planning distributed generations (DGs) and expanding the distribution network systems, embedding a reconfiguration algorithm. However, the reconfiguration task involves a yearly switching operation of distribution feeders i.e. a more frequent switching of feeders is not considered. The work in [17] also uses a static network reconfiguration for the purpose of "mitigating voltage sags and drops" in the presence of distributed energy resources (DERs).

Reference [18] develops a MILP optimization model, incorporating a static network reconfiguration in the presence of wind and energy storage, with the specific aim of reducing the impacts of outages and losses. In [19], network reconfiguration is used to achieve three objectives: minimizing DG curtailments, congestion and voltage rise issues. In a similar line, Ref. [20] investigates the impact of network reconfiguration on the integration level of DGs in distribution systems. Authors in [21] develop a reconfiguration model for increasing the penetration level of plug-in electric vehicles (PEVs) and reducing system costs.

As mentioned earlier, the vast literature in the network reconfiguration area focuses on a static switching of lines, and mainly for the purpose of minimizing network losses and/or improving reliability by balancing load and restoring supply in the event of contingencies. The DNR problem is not adequately addressed from the smart-grids perspective and under high penetration level of variable energy sources. The technological advances make it possible to carry out an hourly (or generally a more frequent) network reconfiguration. This provides a key flexibility option that can partly help to counterbalance the fluctuations in vRESs, and increase their efficient utilization. All this is widely covered in the current work.

The main contributions of this paper are the following:

- The stochastic MILP operational model for dynamic reconfiguration problem of distribution networks in the presence of variable renewable and other distributed energy resources;
- The extensive analysis made with regards to the economic and technical benefits of dynamic reconfiguration, as well as efficient utilization of intermittent power sources.

The remainder of this paper is organized as follows. Section III presents mathematical details of the developed model. Numerical results are discussed in Section IV. The last section concludes the paper.

III. Mathematical Formulation

A. Objective Function

The objective of the formulated DNR problem is to minimize the sum of relevant cost terms, namely, switching costs SWC, expected costs of operation TEC, emissions $TEmiC$ and unserved power $TENSC$ in the system as:

$$Minimize\ TC = SWC + TEC + TENSC + TEmiC \quad (1)$$

where TC refers to the total cost.

A switching cost is incurred when the status of a given line changes from 0 (open) to 1 (closed) or from 1 (closed) to 0 (open). This leads to the absolute value of a difference in successive switching variables. In order to linearly represent such a module, two non-negative auxiliary variables $y_{l,h}^{+}$ and $y_{l,h}^{-}$ are introduced. Thus, SWC can be expressed as a function of the sum of these variables:

$$SWC = \sum_{l\in\Omega^l}\sum_{h\in\Omega^h} SW_l * \left(y_{l,h}^{+} + y_{l,h}^{-}\right) \quad (2)$$

where

$$x_{l,h} - x_{l,h-1} = y_{l,h}^{+} - y_{l,h}^{-};\ y_{l,h}^{+} \geq 0;\ y_{l,h}^{-} \geq 0 \quad (3)$$

$$x_{l,0} = 1;\ \forall l \in \Omega^1\ and\ x_{l,0} = 0;\ \forall l \in \Omega^0 \quad (4)$$

As stated earlier, *TEC* is given by the sum of the cost of power produced by DGs, discharged from energy storage systems (ESSs) and imported from upstream as in (5).

$$TEC = EC^{DG} + EC^{ES} + EC^{SS} \quad (5)$$

where each term in (5) is calculated as:

$$EC^{DG} = \sum_{s\in\Omega^s}\rho_s \sum_{h\in\Omega^h}\sum_{g\in\Omega^g} OC_g P_{g,n,s,h}^{DG} \quad (6)$$

$$EC^{ES} = \sum_{s\in\Omega^s}\rho_s \sum_{h\in\Omega^h}\sum_{es\in\Omega^{es}} \lambda^{es} P_{es,n,s,h}^{dch} \quad (7)$$

$$EC^{SS} = \sum_{s\in\Omega^s}\rho_s \sum_{h\in\Omega^h}\sum_{\varsigma\in\Omega^\varsigma} \lambda_h^{\varsigma} P_{\varsigma,s,h}^{SS} \quad (8)$$

The cost of load shedding *TENSC* is determined as:

$$TENSC = \sum_{s\in\Omega^s}\rho_s \sum_{h\in\Omega^h}\sum_{n\in\Omega^n} (v_{s,h}^{P} P_{n,s,h}^{NS} + v_{s,h}^{Q} Q_{n,s,h}^{NS}) \quad (9)$$

where $v_{s,h}^{P}$ and $v_{s,h}^{Q}$ are penalty parameters corresponding to active and reactive power demand curtailment.

Equation (10) represents the total expected emission cost as a result of power production using DGs and imported power.

$$TEmiC = EmiC^{DG} + EmiC^{SS} \quad (10)$$

where each of the terms in (10) are determined by:

$$EmiC^{DG} = \sum_{s\in\Omega^s}\rho_s \sum_{h\in\Omega^h}\sum_{g\in\Omega^g}\sum_{n\in\Omega^n} \lambda^{CO_2} ER_g^{DG} P_{g,n,s,h}^{DG} \quad (11)$$

$$EmiC^{SS} = \sum_{s\in\Omega^s}\rho_s \sum_{h\in\Omega^h}\sum_{\varsigma\in\Omega^\varsigma}\sum_{n\in\Omega^n} \lambda^{CO_2} ER_{\varsigma}^{SS} P_{\varsigma,s,h}^{SS} \quad (12)$$

B. Constraints

According to Kirchhoff's law, the sum of all incoming flows to a node should be equal to the sum of all outgoing flows. This constraint applies to both active (13) and reactive (14) power flows, and should be respected all the time:

$$\sum_{g\in\Omega^g} P_{g,n,s,h}^{DG} + \sum_{es\in\Omega^{es}} \left(P_{es,n,s,h}^{dch} - P_{es,n,s,h}^{ch}\right) + P_{\varsigma,s,h}^{SS} + P_{n,s,h}^{NS} + \sum_{in,l\in\Omega^l} P_{l,s,h} - \sum_{out,l\in\Omega^l} P_{l,s,h} = PD_{s,h}^{n} + \sum_{in,l\in\Omega^l}\frac{1}{2}PL_{l,s,h} + \sum_{out,l\in\Omega^l}\frac{1}{2}PL_{l,s,h}\ ;\forall\varsigma\epsilon\Omega^{\varsigma};\ \forall\varsigma\epsilon n;\ l\epsilon n \quad (13)$$

$$\sum_{g\in\Omega^g} Q_{g,n,s,h}^{DG} + Q_{c,n,s,h}^{c} + Q_{\varsigma,s,h}^{SS} + Q_{n,s,h}^{NS} + \sum_{in,l\in\Omega^l} Q_{l,s,h} - \sum_{out,l\in\Omega^l} Q_{l,s,h} = QD_{s,h}^{n} + \sum_{in,l\in\Omega^l}\frac{1}{2}QL_{l,s,h} + \sum_{out,l\in\Omega^l}\frac{1}{2}QL_{l,s,h}\ ;\forall\varsigma\epsilon\Omega^{\varsigma};\ \forall\varsigma\epsilon n;\ l\epsilon n \quad (14)$$

The well-known AC power flow equations (which are naturally complex. nonlinear and non-convex functions of voltages and angles) are linearized according to [22]. The linearized active and reactive flows in a line are given by the disjunctive inequalities in (15) and (16), respectively.

$$\left|P_{l,s,h} - \left(V_{nom}\left(\Delta V_{n,s,h} - \Delta V_{m,s,h}\right)g_k - V_{nom}^2 b_k \theta_{l,s,h}\right)\right| \leq MP_l(1 - x_{l,h}) \quad (15)$$

$$\left|Q_{l,s,h} - \left(-V_{nom}\left(\Delta V_{n,s,h} - \Delta V_{m,s,h}\right)b_k - V_{nom}^2 g_k \theta_{l,s,h}\right)\right| \leq MQ_l(1 - x_{l,h}) \quad (16)$$

where MP_l and MQ_l are sufficiently large disjunctive parameters. Moreover, power flows in each line should not exceed the maximum transfer capacity, which is enforced by:

$$P_{l,s,h}^2 + Q_{l,s,h}^2 \leq x_{l,h}(S_l^{max})^2 \quad (17)$$

The following constraints are related to the active (18) and reactive (19) power losses in a line *l*.

$$PL_{l,s,h} = R_l\left(P_{l,s,h}^2 + Q_{l,s,h}^2\right) / V_{nom}^2 \quad (18)$$

$$QL_{l,s,h} = X_l\left(P_{l,s,h}^2 + Q_{l,s,h}^2\right) / V_{nom}^2 \quad (19)$$

Note that the quadratic flows in (17)—(19) are linearized using an SOS2 approach, presented in [23].

Constraints (20)—(25) represent the energy storage model employed in this work. The amount of power charged and discharged are limited as in (20) and (21). Constraint (22) ensures charging and discharging operations do not happen at the same time. The state of charge constraint is given by (23). The storage level should always be within the permissible range as in (24). Equation (25) sets the initial storage level, and makes sure the storage level at the end of the time span is equal to the initial level. For sake of simplicity, both η_{es}^{dch} and η_{es}^{ch} are often set equal (as in the current work).

$$0 \leq P_{es,n,s,h}^{ch} \leq I_{es,n,s,h}^{ch} P_{es,nh}^{ch,max} \quad (20)$$

$$0 \leq P_{es,n,s,h}^{dch} \leq I_{es,n,s,h}^{dch} P_{es,n}^{ch,max} \quad (21)$$

$$I_{es,n,s,h}^{ch} + I_{es,n,s,h}^{dch} \leq 1 \quad (22)$$

$$E_{es,n,s,h} = E_{es,n,s,h-1} + \eta_{es}^{ch} P_{es,n,s,h}^{ch} - P_{es,n,s,h}^{dch}/\eta_{es}^{dch} \quad (23)$$

$$E_{es,n}^{min} \leq E_{es,n,s,h} \leq E_{es,n}^{max} \quad (24)$$

$$E_{es,n,s,h0} = \mu_{es} E_{es,n}^{max}; \; E_{es,n,s,h24} = \mu_{es} E_{es,n}^{max} \quad (25)$$

Equations (26) and (27) impose the active and reactive power limits of DGs, respectively.

$$P_{g,n,s,h}^{DG,min} \leq P_{g,n,s,h}^{DG} \leq P_{g,n,s,h}^{DG,max} \quad (26)$$

$$-\tan\left(cos^{-1}(pf_g)\right) P_{g,n,s,h}^{DG} \leq Q_{g,n,s,h}^{DG} \leq \tan\left(cos^{-1}(pf_g)\right) P_{g,n,s,h}^{DG} \quad (27)$$

The reactive power supplied by switchable capacitor banks (SCBs) is limited by inequality (28):

$$0 \leq Q_{c,n,s,h}^{c} \leq Q_{c,n,s,h}^{c,0} x_{c,n,h} \quad (28)$$

For stability reasons, the reactive power at the substation is subject to bounds as:

$$-\tan\left(cos^{-1}(pf_{ss})\right) P_{\varsigma,s,h}^{SS} \leq Q_{\varsigma,s,h}^{SS} \leq \tan\left(cos^{-1}(pf_{ss})\right) P_{\varsigma,s,h}^{SS}. \quad (29)$$

In addition, distribution networks are normally operated in a radial configuration. Hence, in addition to the aforementioned ones, the radiality constraints in [16] are added to the model in this paper. Furthermore, it should be noted that, in (15) and (16), the angle difference $\theta_{l,s,h}$ is defined as $\theta_{l,s,h} = \theta_{n,s,h} - \theta_{m,s,h}$ where *n* and *m* correspond to the same line *l*.

IV. Numerical Results and Discussions

A. Data and Assumptions

A standard IEEE 41-bus test system, shown in Fig. 1, is employed to test the proposed operational model, and perform the technical and economic analysis of DNR. Details of this test system and further information can be found in [24]. The system has optimally placed distributed energy resources such as wind and solar type DGs, ESSs and SCBs as in [24]. The only exception is at bus 14, where instead of the optimal DG size (3 MW) reported in [24], a 2 MW DG is considered throughout this analysis. Fig. 1 shows the locations of the DGs and ESSs. The time span considered in this work is a 24-hour period, with the possibility of an hourly reconfiguration. The range of permissible voltage deviation at each node is ±5% of the nominal value. The substation is the reference node, whose voltage magnitude and angle are set equal to the nominal value and 0, respectively. Further input data considered in this paper are as follows. Both charging and discharging efficiencies of ESSs is 90%. The power factor at the substation is set constant at 0.8 while the power factor of all DG types is considered to be 0.95. Electricity prices are assumed to follow the same trend as demand, varying between 108 €/MWh during peak and 30 €/MWh during shallow hours. The emission rate at the substation is assumed to be 0.4 tCO_2e/MWh, and the emission rates of solar and wind type DGs are set to 0.0584 and 0.0276 tCO_2e/MWh, respectively. The price of emissions is considered to be 7 €/tCO_2e.

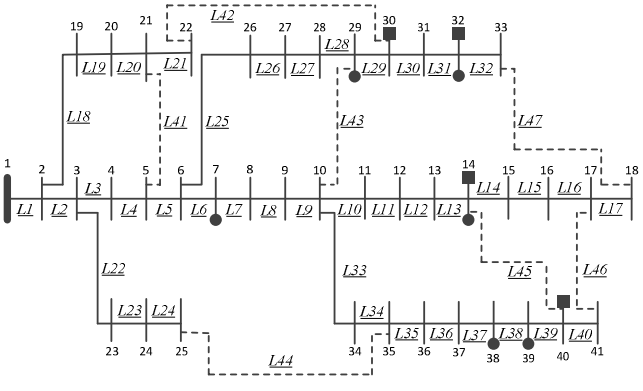

Fig. 1. IEEE 41-bus distribution system with new tie-lines (square and circle dots represent the locations of ESSs and DGs, respectively)

The tariffs of solar and wind power generation are set equal to 40 and 20 €/MWh, respectively. The variable cost of ESSs is considered as 5 €/MWh. The penalty for unserved power (active and reactive alike) is 3000 €/MW. In addition, the power generation profiles of solar and wind type DGs as well as the demand profiles are assumed to be uniform throughout the system. The uncertainty pertaining to demand, wind and solar power outputs are accounted for by considering three different scenarios for each uncertain parameter. It should be noted that each scenario represents an hourly profile of the uncertain parameter under consideration. The combination of the individual scenarios (which in this case are 27) form the new set of scenarios finally considered for the analysis.

B. Discussion of Numerical Results

Four different cases (designated as Case A to D) form part and parcel of the extensive analysis carried out in this work. A summary of the different cases considered in the analysis is shown in Table I. In this table, the control parameters clearly distinguish each case. Case A represents the base case, where there is no reconfiguration and without any DER connected to the system. For this case, the lower bound of voltage is relaxed to avoid unrealistically high unserved power (reactive power, in particular). In Case B, all DERs (DGs, SCBs and ESSs) are connected, but without a dynamic reconfiguration. Case C is similar to Case B but now considering DNR. To further investigate the impacts of DNR on the system's performance and vRES utilization level, Case D is formed, which is similar to the third case but excluding ESSs.

Table II compares the total cost and average losses for the different cases throughout the 24-hours period. As it can be seen in this table, Case A has the highest overall cost and losses

TABLE I. Details of the Considered Cases

Cases	Reconfiguration	DGs	SCBs	ESSs
A	No	No	No	No
B	No	Yes	Yes	Yes
C	Yes	Yes	Yes	Yes
D	Yes	Yes	Yes	No

TABLE II. Costs and Average Losses for Each Case

	Cases			
	A	B	C	D
TC (€)	6526.59	2179.23	2145.09	2741.83
PL (MW)	0.289	0.092	0.068	0.055
QL (MVAr)	0.214	0.075	0.056	0.044

as the demand in the system is met only by importing power through the substation, which is relatively more expensive than local power production using DGs. Note that the losses in Table II are average values; depending on system snapshots, actual losses can be a lot higher. For example, in Case A, active power losses in some operational situations (peak hours) can reach as high as approximately 1 MW. In Case B, losses and costs are slashed each by more than 67% with respective to the values in the base case (i.e. Case A). In Case C, active power losses are further reduced by 26% and system costs by about 2%. Note that the only difference between Case B and C is that the former does not consider reconfiguration but the latter does. Hence, the further reductions in losses and costs in Case C reveal an increased utilization of local power productions (8% more than in Case B). This is as a result of the dynamic reconfiguration considered in Case C. Clearly, DNR enables the system to better manage the variability of vRESs by dynamically and optimally changing the topology to match various operational situations in comparison to a static topology as in Case B. The results of Case D in Table II further demonstrate the positive impacts of dynamic reconfiguration. In this case, ESSs are deliberately not connected to further observe the potential of DNR in scaling up vRES utilization while managing well their imminent side effects. Compared to Cases B and C, total costs in Case D are understandably higher while network losses are surprisingly lower. Yet, the total costs and losses in Case D are substantially lower than that of the base case (by about 58% and 80%, respectively). The slight increase in costs in Case D, in comparison to Cases B and C, is rather expected because unlike in Cases B and C, this one does not have a mechanism to store excess wind or solar power which can be utilized in times of high demand and electricity prices. This obviously leads to a higher cost and a lower overall efficiency in the system. The fact that losses are lower in Case D compared to any other case may be because of the nonexistence of extra flows that would pass through certain lines to be stored.

The results of hourly switching operations corresponding to Cases C and D are summarized in Table III. Note that all other lines that are not shown here do not experience switching operations i.e. the statuses of those lines remain 1 throughout the day. Generally, this table shows more switching operations (in terms of frequency and number of lines "participating" in DNR) in Case D than in Case C. This reveals that, in the absence of a storage medium, the network system tries to

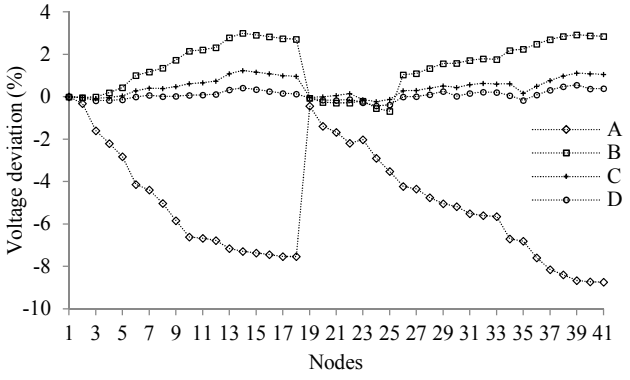

Fig. 2. Average voltage profiles in the system for different cases

TABLE III. RECONFIGURATION OUTCOME OF A TYPICAL DAY.

	Hours with $x_{l,h} = 0$	
	Case C	**Case D**
Line 20	1—3, 5—7, 9, 22—24	8—10, 13—15, 17, 18, 22—24
Line 28	none	1, 3, 4
Line 29	9—21	1—8, 9—16, 24
Line 32	none	2
Line 34	all day long off	all day long off
Line 39	8—13, 17, 18, 22—24	8—10, 18, 22—24
Line 40	none	20, 21
Line 41	4, 8, 10—21	1—7, 11—12, 16, 19, 21
Line 42	1—8, 22—24	9, 17—23
Line 43	all day long off	2, 5—24
Line 45	1—7, 14—16, 19—21	1—7, 11—17, 19—21
Line 46	all day long off	1—19, 22—24
Line 47	all day long off	1, 3—24

efficiently adapt to the continuously changing operational situations, with the aim of routing the actual generation to the nodes where it is being consumed in real-time. For example, line L44 is always turned on in order to interconnect the demand nodes with the RES nodes. Dynamically switching line L45 seems to pave the way to easily ship excess power productions to the demands connected at either side of this line. Line L42 increases the flexibility of partly meeting the demand at node 21 and its vicinity by routing local power production from the wind reach nodes 29 and 32. Generally, DNR leads to a more efficient operation of the system.

Fig. 2 plots the average voltage profiles in the system for all cases. Note that this figure displays only the average values; in some operational situations, in the base case, voltage deviations at the farthest nodes can be as high as 18%. The voltage profile of the base case indicates that the system is highly lossy and poorly compensated. As a result, voltages at most of the nodes exceed the technically permissible limit (5%). Furthermore, by closely studying the voltage profiles in Fig. 2, one can observe the dramatic impact of optimally placed DERs (DGs, ESSs and SCBs in this case). In addition, the positive contribution of DNR in improving the voltage profile in the system is also evident in this figure by comparing the profiles corresponding to Cases B and C (see the first and the second curves from above). Compared to Case B (where a static topology is considered), Case C leads to a largely smoother voltage profile, and the voltage in every node is closer to the nominal value.

Generally, the analysis here clearly shows the substantial benefits DNR in terms of providing more flexibility to the system, which is highly desired to integrate and efficiently utilize a large quantity of intermittent power at distribution levels. DNR enables the system to better adapt to continuously changing situations, and distribute the locally produced "cleaner" power to the demand while meeting all technical requirements.

Fig. 3 presents the energy mix corresponding to Case C. This shows that more than 90% of the electricity demand in the system is met by energy that comes from wind and solar type DGs. A small quantity of electricity is imported only during valley hours (when the electricity price is low) mainly to

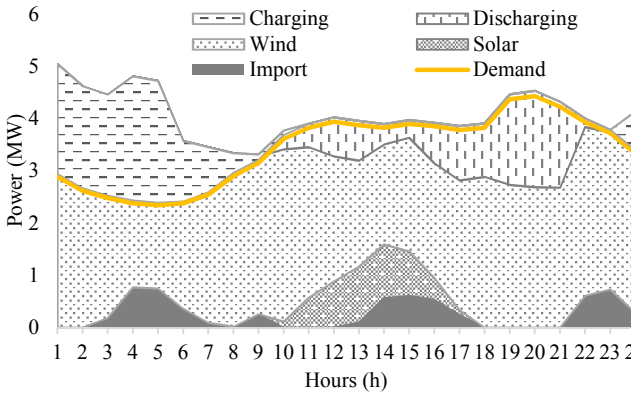

Fig. 3. Energy mix in Case C

charge the ESSs in the system, and during peak hours to meet the portion of demand that could not be locally supplied.

V. Conclusions

This paper has proposed a stochastic MILP optimization model to investigate the impacts of DNR in the smart grids context featuring a significant amount of distributed energy resources, particularly, wind and solar type DGs, ESSs and reactive power sources. The optimization problem, which is based on a linearized AC network model, minimizes the sum of the most relevant cost terms subject to a number of technical and economic constraints. In a dynamic operation framework, the proposed model delivers multiple optimal topologies of the existing network system that fits well with the system's varying hourly operational conditions. Numerical results generally show that DNR leads to a more efficient utilization of renewable type DGs integrated in the system, reduced costs and losses, and a substantially improved system performance especially the voltage profile in the system.

References

[1] J. Yan, T. Shamim, S. K. Chou, U. Desideri, and H. Li, "Clean, efficient and affordable energy for a sustainable future," Appl. Energy, Jun. 2016.

[2] Renewables 2015 - Global Status Report, Renewable Energy Policy Network for the 21st Century. .

[3] A. Aslani, P. Helo, and M. Naaranoja, "Role of renewable energy policies in energy dependency in Finland: System dynamics approach," Appl. Energy, vol. 113, pp. 758–765, Jan. 2014.

[4] V. Krakowski, E. Assoumou, V. Mazauric, and N. Maïzi, "Feasible path toward 40–100% renewable energy shares for power supply in France by 2050: A prospective analysis," Appl. Energy, vol. 171, pp. 501–522, Jun. 2016.

[5] P. S. Georgilakis and N. D. Hatziargyriou, "Optimal Distributed Generation Placement in Power Distribution Networks: Models, Methods, and Future Research," IEEE Trans. Power Syst., vol. 28, no. 3, pp. 3420–3428, Aug. 2013.

[6] O. Badran, S. Mekhilef, H. Mokhlis, and W. Dahalan, "Optimal reconfiguration of distribution system connected with distributed generations: A review of different methodologies," Renew. Sustain. Energy Rev., vol. 73, pp. 854–867, Jun. 2017.

[7] B. Sultana, M. W. Mustafa, U. Sultana, and A. R. Bhatti, "Review on reliability improvement and power loss reduction in distribution system via network reconfiguration," Renew. Sustain. Energy Rev., vol. 66, pp. 297–310, Dec. 2016.

[8] D. Q. Hung and N. Mithulananthan, "Loss reduction and loadability enhancement with DG: A dual-index analytical approach," Appl. Energy, vol. 115, pp. 233–241, Feb. 2014.

[9] S. M. M. Larimi, M. R. Haghifam, and A. Moradkhani, "Risk-based reconfiguration of active electric distribution networks," Transm. Distrib. IET Gener., vol. 10, no. 4, pp. 1006–1015, 2016.

[10] H.-C. Chang and C.-C. Kuo, "Network reconfiguration in distribution systems using simulated annealing," Electr. Power Syst. Res., vol. 29, no. 3, pp. 227–238, May 1994.

[11] C.-T. Su, C.-F. Chang, and J.-P. Chiou, "Distribution network reconfiguration for loss reduction by ant colony search algorithm," Electr. Power Syst. Res., vol. 75, no. 2–3, pp. 190–199, Aug. 2005.

[12] M. R. Dorostkar-Ghamsari, M. Fotuhi-Firuzabad, M. Lehtonen, and A. Safdarian, "Value of Distribution Network Reconfiguration in Presence of Renewable Energy Resources," IEEE Trans. Power Syst., vol. 31, no. 3, pp. 1879–1888, May 2016.

[13] I.-K. Song, W.-W. Jung, J.-Y. Kim, S.-Y. Yun, J.-H. Choi, and S.-J. Ahn, "Operation Schemes of Smart Distribution Networks With Distributed Energy Resources for Loss Reduction and Service Restoration," IEEE Trans. Smart Grid, vol. 4, no. 1, pp. 367–374, Mar. 2013.

[14] D. Q. Hung, N. Mithulananthan, and R. C. Bansal, "A combined practical approach for distribution system loss reduction," Int. J. Ambient Energy, vol. 36, no. 3, pp. 123–131, May 2015.

[15] R. Rajaram, K. Sathish Kumar, and N. Rajasekar, "Power system reconfiguration in a radial distribution network for reducing losses and to improve voltage profile using modified plant growth simulation algorithm with Distributed Generation (DG)," Energy Rep., vol. 1, pp. 116–122, Nov. 2015.

[16] G. Munoz-Delgado, J. Contreras, and J. M. Arroyo, "Joint Expansion Planning of Distributed Generation and Distribution Networks," IEEE Trans. Power Syst., vol. 30, no. 5, pp. 2579–2590, Sep. 2015.

[17] A. Asrari, T. Wu, and S. Lotfifard, "The Impacts of Distributed Energy Sources on Distribution Network Reconfiguration," IEEE Trans. Energy Convers., vol. 31, no. 2, pp. 606–613, Jun. 2016.

[18] P. Meneses de Quevedo, J. Contreras, M. J. Rider, and J. Allahdadian, "Contingency Assessment and Network Reconfiguration in Distribution Grids Including Wind Power and Energy Storage," IEEE Trans. Sustain. Energy, vol. 6, no. 4, pp. 1524–1533, Oct. 2015.

[19] N. C. Koutsoukis, D. O. Siagkas, P. S. Georgilakis, and N. D. Hatziargyriou, "Online Reconfiguration of Active Distribution Networks for Maximum Integration of Distributed Generation," IEEE Trans. Autom. Sci. Eng., vol. PP, no. 99, pp. 1–12, 2016.

[20] F. Capitanescu, L. F. Ochoa, H. Margossian, and N. D. Hatziargyriou, "Assessing the Potential of Network Reconfiguration to Improve Distributed Generation Hosting Capacity in Active Distribution Systems," IEEE Trans. Power Syst., vol. 30, no. 1, pp. 346–356, Jan. 2015.

[21] A. Kavousi-Fard, A. Abbasi, M.-A. Rostami, and A. Khosravi, "Optimal distribution feeder reconfiguration for increasing the penetration of plug-in electric vehicles and minimizing network costs," Energy, vol. 93, Part 2, pp. 1693–1703, Dec. 2015.

[22] S. F. Santos, D. Z. Fitiwi, M. Shafie-Khah, A. W. Bizuayehu, C. M. P. Cabrita, and J. P. S. Catalão, "New Multistage and Stochastic Mathematical Model for Maximizing RES Hosting Capacity - Part I: Problem Formulation," IEEE Trans. Sustain. Energy, vol. 8, no. 1, pp. 304–319, Jan. 2017.

[23] D. Z. Fitiwi, L. Olmos, M. Rivier, F. de Cuadra, and I. J. Pérez-Arriaga, "Finding a representative network losses model for large-scale transmission expansion planning with renewable energy sources," Energy, vol. 101, pp. 343–358, Apr. 2016.

[24] S. F. Santos, D. Z. Fitiwi, M. Shafie-khah, A. W. Bizuayehu, C. M. P. Cabrita, and J. P. S. Catalão, "New Multi-Stage and Stochastic Mathematical Model for Maximizing RES Hosting Capacity - Part II: Numerical Results," IEEE Trans. Sustain. Energy, vol. 8, no. 1, pp. 320–330, Jan. 2017.